

# Affects of graphite morphology and matrix structure on mechanical properties of cast irons

JAW-MIN CHOU, MIN-HSIUNG HON

*Department of Materials Engineering, National Cheng Kung University, Tainan, Taiwan*

JYE-LONG LEE

*Steel and Aluminum R and D Department, China Steel Corporation, Kaohsiung, Taiwan*

A comparative study of the affects of graphite morphology and matrix structure on mechanical properties was carried out on spheroidal, compacted and flake graphite irons by a short austenitizing plus austempering treatment. Transformation kinetic data showed that compacted graphite iron had the fastest, spheroidal graphite iron the second and flake graphite iron the slowest austenitizing rate. In spheroidal and compacted graphite irons the strength increased, while ductility decreased, with increasing the amount of bainite in matrix due to prolonging austenitizing time. On the other hand, the increase of bainite structure in the matrix had no significant affect on the mechanical properties of flake graphite iron. Fractographic examinations showed that the fracture surface of spheroidal graphite iron changed from a ductile mode to a brittle mode when its matrix changed from ferrite to bainite dominant. The flake graphite iron ruptured with brittle mode no matter what matrix it had. Compacted graphite iron exhibited an intermediate type of fracture surface. With a short austenitizing plus austempering treatment, the mechanical properties of spheroidal and compacted graphite irons could be improved and extended to a very wide range.

## 1. Introduction

The influence of graphite morphology on mechanical and thermal properties has long been a subject for the study of cast irons [1-3]. Spheroidal cast graphite iron has been developed to provide superior strength and ductility in addition to the well-known grey iron, which is characterized by flake graphite and excellent thermal conductivity. In the past few years, compacted graphite iron [2, 4, 5] has received considerable attention due to its good combination of mechanical and thermal properties.

On the other hand, the structure of the matrix also has a great influence on the properties of cast iron [6, 7]. A number of thermal processes have been developed to modify the matrix structure and thus the properties of cast iron [6-8]. Among these processes, austempering is widely used to improve the strength of spheroidal graphite iron. In addition, a short austenitizing treatment plus austempering [9] has also been employed to produce a mixed ferrite-bainite matrix which has a fairly wide range of mechanical properties. However, the affects of both the above two treatments on the structure and mechanical properties of flake and compacted graphite irons have not been extensively investigated. The influence of matrix structure of austempered iron with different graphite morphology on mechanical properties is therefore difficult to understand.

In the present study, flake, compacted, and spheroidal graphite irons were submitted to austenitizing

and then austempering to produce a matrix with various combinations of ferrite and bainite. Transformation kinetics and mechanical properties were also examined. An attempt is made to realize the affects of graphite morphology and matrix structure on the mechanical properties of cast irons.

## 2. Experimental procedures

### 2.1. Materials

The cast iron used in this study was prepared with commercial pig iron by induction melting. Three 70 kg melts were treated with 0, 0.65 and 1.3% Fe-8.6wt% Mg-47wt% Si spheroider, respectively. After spheroidization treatment, the melt was cast into a Y block, the dimensions of which are shown in Fig. 1. The chemical compositions of the cast irons are listed in Table I.

### 2.2. Heat treatments

All castings were subjected to a ferritization treatment to obtain a full ferrite matrix before austempering. Before austenitizing, specimens were reheated at 680°C for 20 min. to ensure a uniform specimen temperature. The specimens were then austenitized at 950°C and held for 20, 40, 80, 120, 600, 1800 and 3600 sec, respectively. In order to prevent the specimens oxidizing the austenitizing treatment was carried out in a salt bath. Following austenitization, specimens were quickly transferred to another salt bath and austempered at 420 and 320°C, respectively, for 1 h.

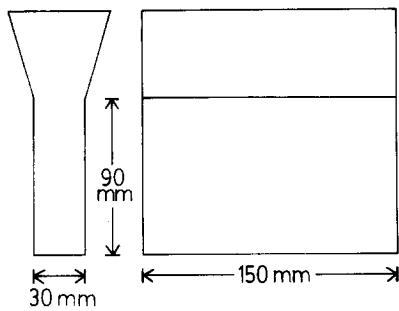


Figure 1 The dimensions of the Y block.

### 2.3. Tensile tests

After austempering, specimens were subjected to the tensile test. Data collected from each specimen included ultimate tensile strength, 0.2% offset yield strength and percentage elongation. Each datum was the average of two tensile tests.

### 2.4. Metallography

Metallographic examination was carried out by using an optical microscopy (OM) after the specimens had been ground, polished and etched with 2% Nital. The volume fraction of ferrite in the matrix was measured by an image analyzer. Each datum obtained was the average of at least 15 areas of dimensions  $950 \times 800 \mu\text{m}^2$ . The morphology of bainite examined by scanning electron microscopy (SEM).

The fracture surface was removed from the tensile specimens after tensile tests, and the fractographs were examined by SEM.

## 3. Results and discussion

### 3.1. Graphite morphology

To evaluate the affect of graphite morphology on the mechanical properties of cast irons, different amounts of spheroider were added to three melts and thereby three types of cast iron as shown in Fig. 2, i.e. flake, compacted, and spheroidal graphite cast irons, were obtained. According to Evans *et al.* [1, 10, 11], the change of graphite morphology essentially results from the difference in residual magnesium content in cast irons. This can be confirmed by Table I where the magnesium content is greatest spheroidal graphite iron, then compacted iron and lowest in flake graphite iron.

### 3.2. Transformation kinetics

Fig. 3a shows the ferrite volume fraction in matrix ( $X\%$ ) plotted against austenitizing time after the specimens have been austenitized at  $950^\circ\text{C}$  for various times and then austempered at  $320^\circ\text{C}$  for 1 h. In all three irons the volume fraction of ferrite decreases with increasing austenitizing time. It is reasonable that prolonging austenitizing allows carbon atoms to

travel farther from the graphite and make more ferrite transform to austenite. Consequently, more matrix would transform to bainite after austempering.

Fig. 3a also shows that the time needed to achieve full austenitization is about 100, 120 and 500 sec for compacted, spheroidal and flake cast graphite irons, respectively. This result seems some what peculiar since most of the thermal and mechanical properties of compacted iron have been reported [1–5] to exist between spheroidal and flake graphite irons. It is well known that in graphite the carbon atoms stack as a hexagonal closed packed (h c p) crystal. Many investigators [11–13] have proposed that in spheroidal graphite the carbon atoms are deposited predominantly along the C axis of the h c p crystal, while in flake graphite the deposition direction of carbon atom is mainly along the A axis. The atomic bondings between neighbouring atoms are Van Der Waals force along the C axis and covalent along the A-axis. The energy required to break the bonding between the atoms is certainly lower in the C-axis than in the A-axis [14]. Carbon atoms in spheroidal graphite iron, therefore, diffuse away from graphite more easily than do atoms in flake graphite iron. Carbon atoms in compacted graphite iron are also believed [15–17] to stack dominantly along the C-axis, which in turn favours the separation of carbon atoms from graphite. It is comprehensible from the above energy consideration that the transformation rate of spheroidal and compacted graphite iron is faster than that of flake graphite iron. However, the difference in transformation kinetics between spheroidal and compacted graphite irons seems difficult to understand with the above model. The difference in the transformation rates of spheroidal and compacted graphite iron may simply have arisen from the difference in the surface area of the graphites. From the geometric view point, the surface area of compacted graphite is larger than that of spheroidal graphite. Therefore, the available sites for carbon atoms to diffuse away from are larger on the surface of compacted graphite than on the spheroidal graphite. As a result, the austenitization of compacted graphite iron is faster than spheroidal graphite iron.

The transformation kinetics for irons austempered at  $420^\circ\text{C}$  is shown in Fig. 3b. The amount of ferrite also decreases with increasing austenitizing time. The compacted graphite still has the fastest transformation rate and the flake graphite the slowest transformation. From the results in Figs 3a and b, it is clear that graphite morphology has an affect on the transformation kinetics of irons.

### 3.3. Microstructure

Fig. 4 shows the microstructural change of spheroidal

TABLE I Chemical composition of cast irons

	C (wt %)	Si (wt %)	Mn (wt %)	P (wt %)	S (wt %)	Mg (wt %)
Spheroidal graphite iron	3.51	2.49	–	0.033	0.015	0.0384
Compacted graphite iron	3.51	2.52	0.003	0.031	0.013	0.0187
Flake graphite iron	3.56	2.51	0.008	0.026	0.035	–

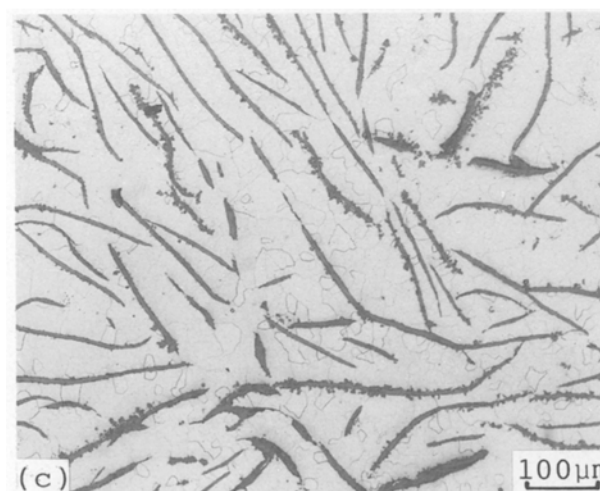
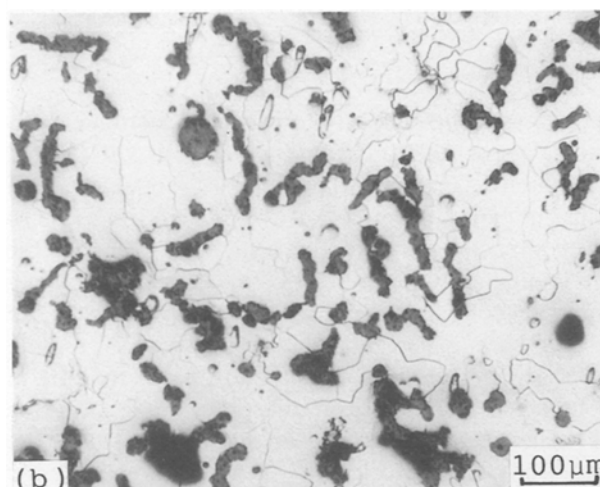
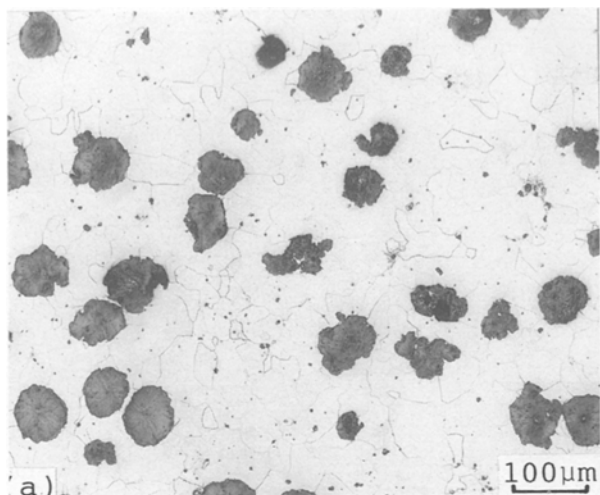


Figure 2 Optical micrographs of cast irons (a) spheroidal graphite iron (b) compacted graphite iron (c) flake graphite iron.

graphite iron with increasing austenitizing time. When the iron was austenitized for 20 sec, only a shell of bainite which surrounds the graphite can be seen (Fig. 4a). The shell thickness with increasing austenitizing time at the expense of ferrite matrix (Figs 4b and c). This trend of structural change is consistent with the kinetic data. Metallographic examination of structural change in compacted and flake graphite iron also showed good agreement with

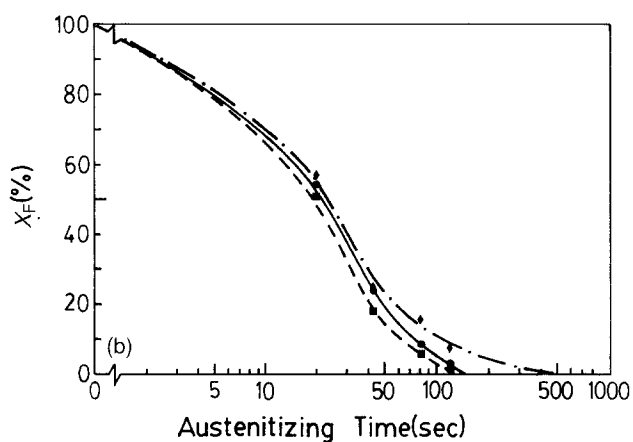
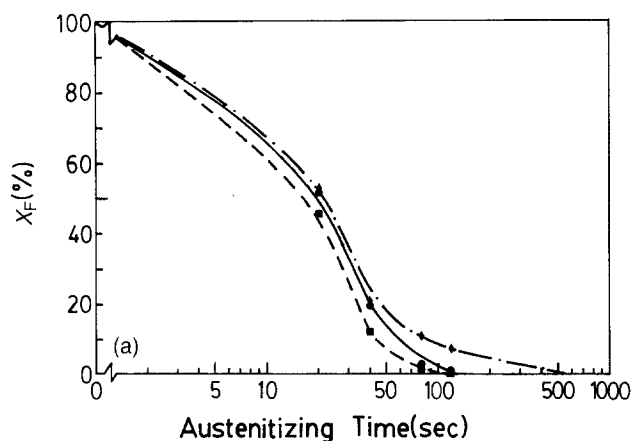


Figure 3 Affect of austenitizing time on the ferrite volume fraction of spheroidal (SG) (—●—), compacted (CG) (---■---), and flake graphite (FG) (-·-◆-) iron. (a) austempered at 320°C (b) austempered at 420°C.

the kinetic data. The shell of hard structure surrounding the spheroidal graphite has also been reported by Okabayashi *et al.* [18, 19]. They referred to such a structure as “hard eyes”. In compacted and flake graphite irons, however, the structure after short austenitizing treatment and the austempering was hardly mentioned. Fig. 5 shows micrographs at a higher magnification of three irons that were briefly austenitized. It can be seen that there is also a shell of bainite surrounding the compacted graphite (Fig. 5b) and all the bainite in compacted and spheroidal graphite irons is in intimate contact with graphites (Figs 5a and b). On the other hand, the bainite in flake graphite iron is not regularly distributed and graphites are not always enveloped by the bainite (Fig. 5c). This finding suggests that compacted and spheroidal graphites have more available sites for carbon to diffuse away from the flake graphite, and thus is in good agreement with theoretical predictions mentioned previously. It can be, therefore, be realized that the faster transformation rate in compacted and spheroidal graphite irons obviously results from more available diffusion sites for carbon on the surface of graphite.

### 3.4. Mechanical properties

The results of tensile tests of three irons are shown in Fig. 6 in which tensile strength (TS), yield strength (YS) and elongation (E) are plotted against austenitizing

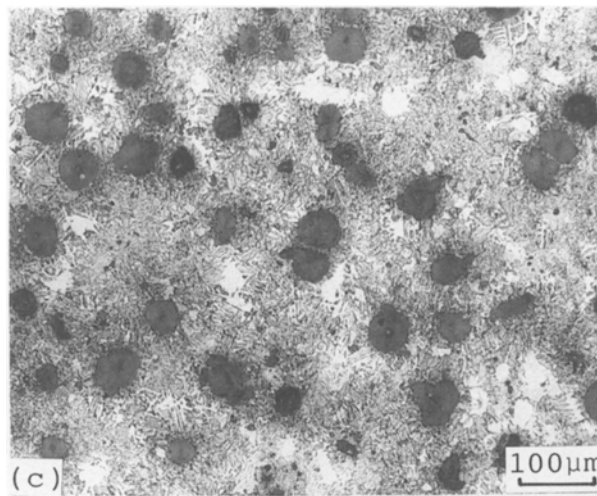
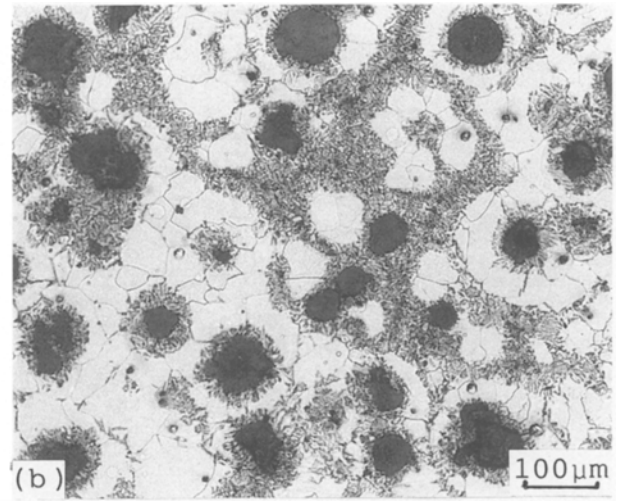
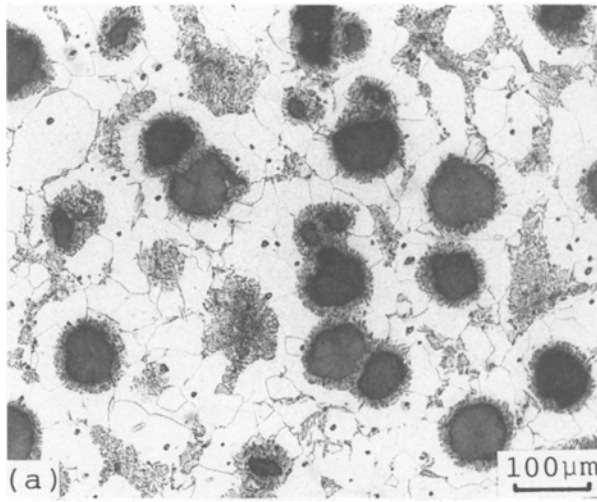


Figure 4 Optical micrographs of spheroidal graphite iron austenitized for (a) 20 sec, (b) 40 sec, (c) 80 sec.

time. Both tensile strength and yield strength of spheroidal and compacted graphite irons increase quickly with increasing austenitizing time at first and then level off at about 120 sec (Fig. 6a). From the kinetic results and metallographic observations in previous sections, it is easy to see that the increase in strength is the result of increasing volume fraction of bainite in the matrix. In addition, the level-off time happens to be consistent with the time required for full austenitization of the matrix. This means that once the matrix had been fully austenitized a further increase in austenitizing time had no significant influence on the strength. By contrast, elongation of spheroidal and compacted graphite irons decreases with increasing austenitization up to about 120 sec. It is reasonable when the soft structure (ferrite) in matrix decreases and the hard structure (bainite) increases, the ductility of the iron should decrease. Therefore, so far as compacted and spheroidal graphite irons are concerned, the structure of the matrix is the dominant factor in controlling the mechanical properties of the irons. Inspection of the whole range of austenitizing treatment (Fig. 6a), shows that the strength of spheroidal graphite iron is higher than that of compacted iron except in the interval of 20 to 40 sec, in which compacted graphite iron exhibits a higher strength than spheroidal graphite iron. It is well known that spheroidal graphite iron is always stronger than compacted graphite iron if both irons have the same matrix structure [2]. The

above result was unlikely to have arisen from experimental error since austempering at both 320°C (Fig. 6a) and 420°C (Fig. 6b) exhibited a similar result. It must be borne in mind that the austenitizing rate of the compacted graphite iron is slightly faster than the spheroidal graphite iron. At 20 to 40 sec austenitizing interval, compacted graphite iron has a matrix of higher bainite percentage than spheroidal graphite iron. The higher volume fraction of hard structure in compacted graphite iron must be the reason for the unexpected difference in strength between the two irons. This result can further demonstrate the importance of the structure of the matrix in determining the strength of spheroidal and compacted graphite irons. Throughout the whole austenitizing treatment range the elongation of compacted graphite iron is never greater than that of spheroidal graphite iron.

For flake graphite iron, neither strength nor ductility significantly changes throughout the whole range of austenitizing treatment, even if the matrix entirely transforms to bainite. Therefore, in flake graphite iron, the matrix structure has little effect on the mechanical properties.

Different times at austenitizing temperature and then austempering at 320°C (Fig. 6a) enables the mechanical properties of spheroidal graphite iron to be extended over a very wide range, from high ductility level (TS = 400 MPa, E(%) = 25 untreated specimen) to good strength-ductility balance (TS = 630 MPa E(%) = 14 at austenitizing time = 20 sec) and to high strength level (TS = 1300 MPa E(%) = 5 at austenitizing time = 120 sec). If spheroidal graphite iron was austempered at 420°C, a good strength-ductility combination of about TS = 540 MPa and E(%) = 17.5 at 20 sec austenitizing time = could be obtained. The very high strength level achieved by 320°C austempering is believed to be chiefly due to the presence of lower bainite which exhibits an extremely fine bainitic plate as shown in Fig. 7a. The good strength-ductility balance obtained by 420°C austempering is as a result of the formation of upper bainite (Fig. 7b) which exhibits a coarse bainite lath and contains a fairly high portion of retained austenite. The improve-

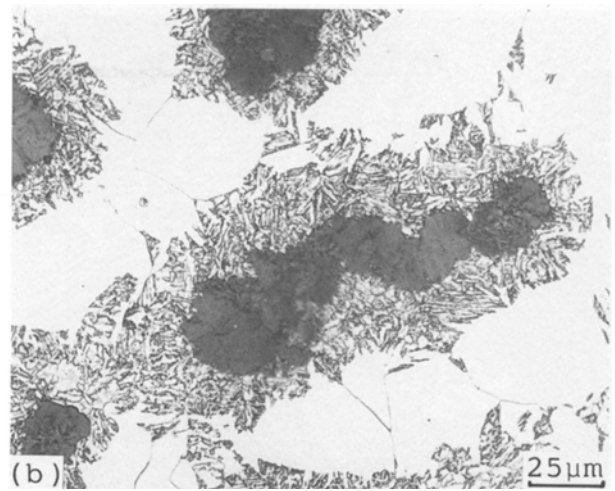
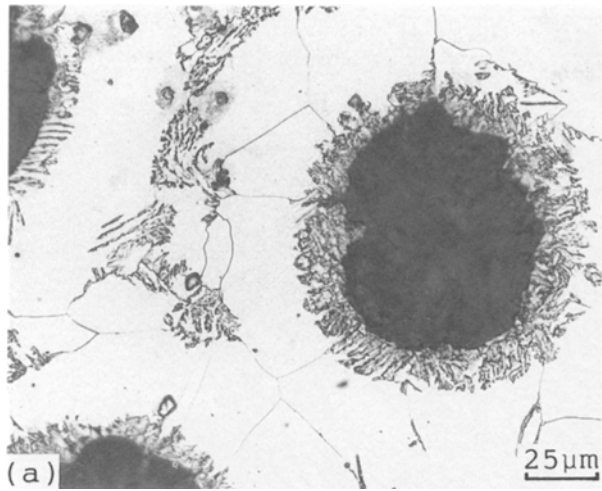


Figure 5 Optical micrographs of cast irons austenitized 20 sec at 950°C. (a) spheroidal graphite iron (b) compacted graphite iron (c) flake graphite iron.

ment in strength level or strength-toughness balance makes spheroidal iron more capable of used in a critical situation and more competitive with other engineering materials.

Austempering also greatly improves the mechanical properties of compacted graphite iron. Austempering followed by a complete austenitizing treatment can make compacted graphite iron achieve a tensile strength of more than 1100 MPa; that is three times as high as the ferritic compacted graphite iron. The same short austenitizing treatment followed by austempering can make the compacted graphite even

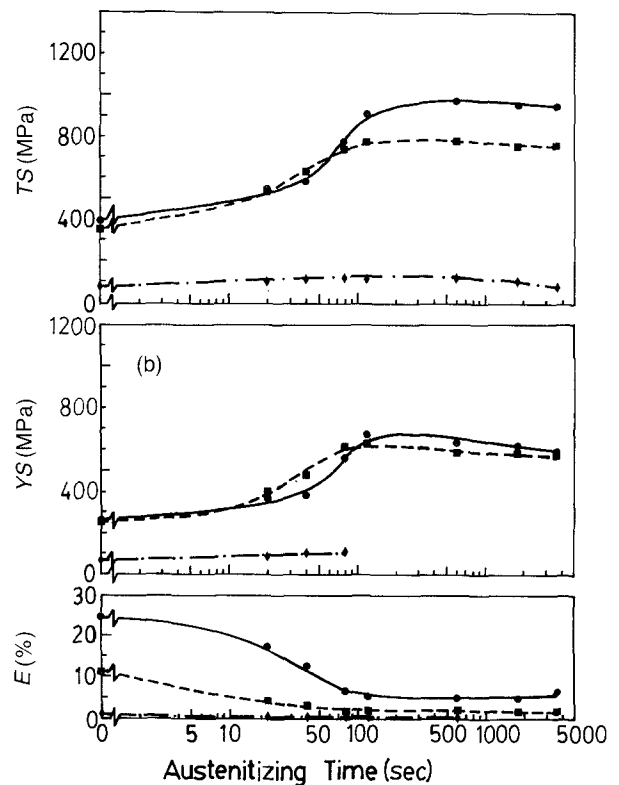
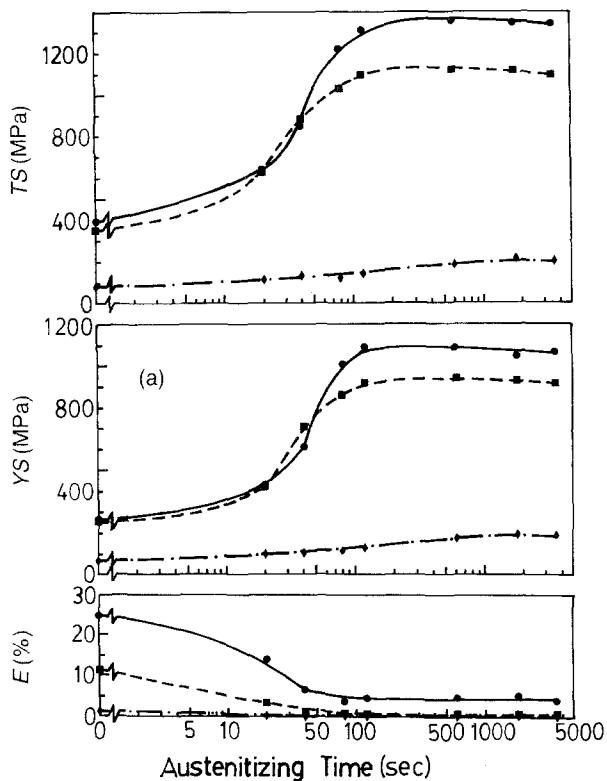


Figure 6 Effect of austenitizing time on the tensile properties of spheroidal (SG) (—●—), compacted (CG) (—■—), and flake graphite (FG) (—◆—) iron. (a) austempered at 320°C (b) austempered at 420°C.

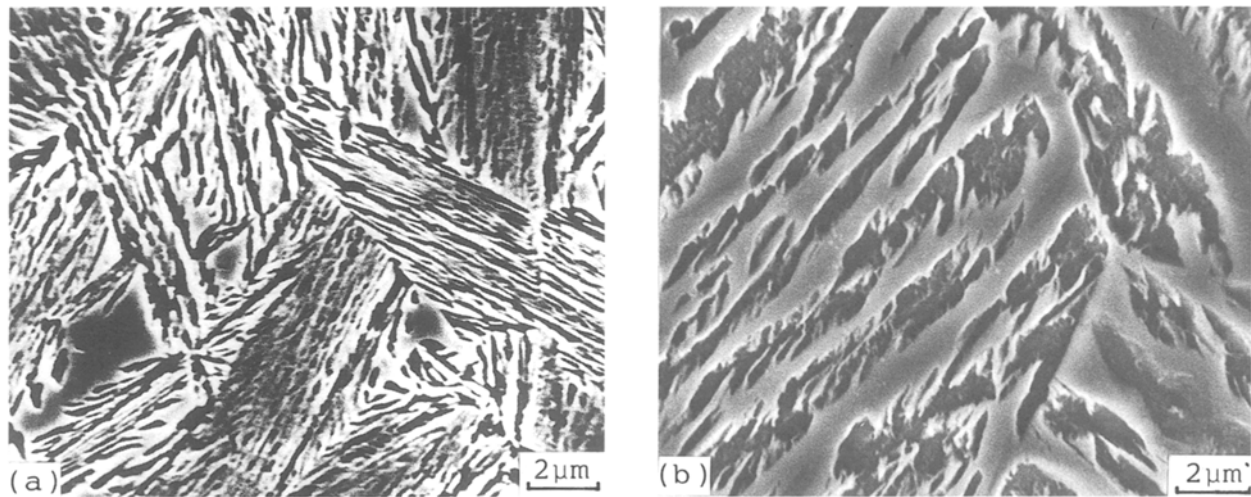


Figure 7 SEM micrographs of spheroidal graphite iron austenitized 1 h at 950°C. (a) austempered at 320°C (b) austempered at 420°C.

stronger than spheroidal graphite iron. As well as the excellent heat conductivity reported in compacted graphite [1, 2], the above result shows that austempering compacted graphite iron has a great potential for environmental use where a good strength-heat conductivity balance is required and where spheroidal graphite iron is not suitable because of its poor heat conductivity [1, 2]. In the case of flake graphite iron, austempering hardly improves the mechanical properties.

### 3.5. Fractography

Analysis of fracture surfaces illuminates the effect of graphite morphology and matrix structure on ductility. The fracture surfaces of specimens austenitized for various times are shown in Fig. 8. In spheroidal graphite iron, a dominant ductile very dimpled fracture surface was observed for the specimen austenitized for 20 sec (Fig. 8a) and thus having a matrix of about 55% ferrite and 45% bainite. Considerable localized cleavage can be seen in the specimen with more than 90% bainite matrix as shown in Fig. 8b. After further austenitization, the cleavage surface became dominant (Fig. 8c) because the whole matrix had already been transformed to bainite. The above results lead to the conclusion that in spheroidal graphite iron when the matrix changes from ferrite to bainite dominant the fracture surface will change from ductile to brittle mode. This is consistent with the results of mechanical properties tests, in which a spheroidal graphite iron with a high ferrite matrix exhibited high ductility.

With the same heat treatment, compacted graphite iron always exhibits a higher proportion of cleavage surface than spheroidal graphite iron (Figs 8d to f). Some regions of cleavage surface can be seen even in the specimen austenitized for just 20 sec (Fig. 8d) and having a matrix of about 50% ferrite. Rupture with more cleavage mode always makes the ductility of compacted iron lower than that of spheroidal iron (Fig. 6). All specimens of flake iron have a brittle fracture surface as shown in Figs 8g to i, even in the specimen austenitized for just 20 sec, no obvious dimple can be seen (Fig. 8g). The low ductility of flake

graphite iron (Fig. 6) is, therefore, due to rupture with brittle mode.

From the fractographic observations, it can be pointed out that no matter how large a proportion of ductile phase (ferrite) there is in the matrix, flake graphite iron always ruptures with brittle mode, while in spheroidal and compacted graphite irons ductile fracture surface increases with increasing ductile phase in the matrix. The dependence of fracture mode on the structure of the matrix can be explained as follows. In flake graphite iron, graphites are interconnected [20]. Once a crack is initiated, it prefers to propagate along the weakest structure, i.e. graphites. The crack propagating along the interconnected graphites does not need to overcome the fracture resistance of the matrix. Thus, the ductility and fracture mode are independent of the structure of the matrix. In spheroidal graphite iron, graphites exist individually and are surrounded by the matrix. When the crack propagates from one graphite nodule to the other, it must cross the matrix. Hence the structure of the matrix certainly plays an important role in the resistance of the propagation of the crack. From the microstructural study of compacted graphite iron, it is observed that the graphite is thick, with rounded edges, and is intermediate in shape between the flake graphite and spheroidal graphite [2-5, 21]. The fracture behaviour and thus the ductility of compacted graphite iron behaves, therefore, as a mixed mode of spheroidal and flake graphite irons.

### 4. Conclusions

A comparative study of the effects of graphite morphology and matrix structure on the mechanical properties was carried out in spheroidal, compacted, and flake graphite irons by a short austenitization plus austempering treatment. The major conclusions are summarized as follows.

(1) The austenitizing rate was fastest in compacted graphite iron, then spheroidal graphite iron and slowest in flake graphite iron.

(2) The tensile strength of both spheroidal and compacted graphite irons increased rapidly with increasing austenitizing time and then levelled off at about



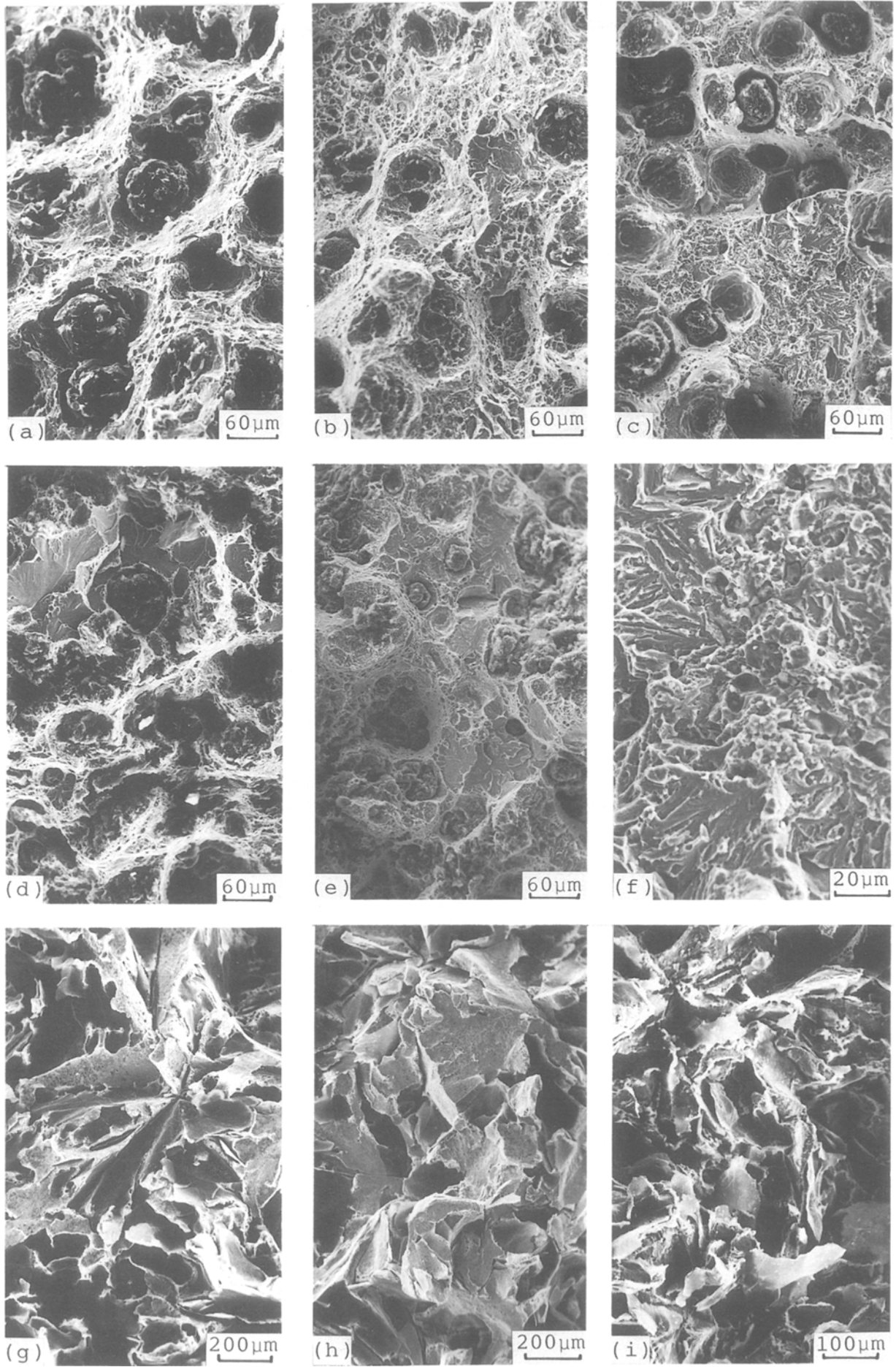


Figure 8 Fractographs of austenitized cast irons. Spheroidal graphite iron (a) 20 sec, (b) 80 sec, (c) 3600 sec. Compacted graphite iron (d) 20 sec, (e) 80 sec, (f) 3600 sec. Flake graphite iron (g) 20 sec, (h) 80 sec, (i) 3600 sec.

120 sec which was consistent with the time required to achieve a full austenitization, while ductility of both irons decreased with increasing austenitizing time. The change of mechanical properties was chiefly due to the presence of various amounts of bainite in the matrix. Under the present experimental conditions, most spheroidal graphite iron specimens were stronger than the compacted graphite iron specimens except for 20 to 40 seconds austenitizing, where compacted graphite iron exhibited a higher strength than the spheroidal graphite iron due to a higher fraction of bainite in the matrix.

(3) An increase in the austenitizing time and thus an increase in the bainite fraction in the matrix did not significantly affect the mechanical properties of flake graphite iron.

(4) Fractographic examinations showed that the fracture surface of the spheroidal graphite iron changed from a ductile mode to a brittle one when its matrix changed from ferrite to bainite dominant, flake graphite iron, however, always ruptured with brittle mode on matter what matrix it had. The fracture surface of compacted graphite iron was intermediate between spheroidal and flake irons.

(5) With a short austenitizing plus austempering treatment, the mechanical properties of spheroidal and compacted graphite irons could be extended to a very wide range from a high ductility level to a good ductility-strength balance and to a high strength.

(6) For 20 sec austenitizing, a shell of bainite was developed surrounding spheroidal and compacted graphites, while bainite was not uniformly distributed around the flake graphite iron. This phenomenon was due to there being more available in spheroidal and compacted graphite irons than in flake graphite iron for carbon to diffuse from.

## References

1. E. R. EVANS, J. V. DAWSON and M. J. LALICH, *AFS Trans.* **84** (1976) 215.
2. R. W. MONROE and C. E. BATES, *ibid.* **90** (1982) 615.
3. V. S. R. MURTHY and S. SESHAN, *ibid.* **92** (1984) 373.
4. J. POWELL, *The British Foundryman* **77** (1984) 472.
5. V. S. R. MURTHY, KISHORE and S. SESHAN, *ibid.* **78** (1985) 71.
6. J. F. JANOWAK and R. B. GUNDLACH, *J. Heat Treating* **4** (1985) 25.
7. J. F. JANOWAK, R. B. GUNDLACH, G. T. ELDIS and K. ROHRIG, *AFS Inter. Cast Metals J.* **6** (1981) 28.
8. P. S. COWEN, *Foundry* **99** (1971) 60.
9. N. WADE and Y. UEDA, *Trans. ISIJ* **21** (1981) 117.
10. J. V. DAWSON and E. R. EVANS, *BCIRA J.* **22** (1974) 137.
11. R. H. McSWAIN and C. E. BATES, *AFS Inter. Cast Metals J.* **1** (1976) 53.
12. B. LUX, *ibid.* **18** (1972) 25.
13. C. R. LOPER, R. C. VOIGT, J. R. YANG and G. X. SUN, *AFS Trans.* **89** (1981) 529.
14. R. H. McSWAIN and C. E. BATES in "The Metallurgy of Cast Iron". (Georgi Publishing Co., Switzerland, 1974) p. 423.
15. P. C. LIU, C. R. LOPER, Jr., T. KIMURA and H. K. PARK, *AFS Trans.* **88** (1980) 97.
16. P. C. LIU, C. R. LOPER, Jr., T. KIMURA and E. N. PAN, *ibid.* **89** (1981) 65.
17. N. N. ALEKSANDROV, B. S. MIL'MAN, N. G. OSAKA, L. V. IL'ICHEVA and V. V. VANDREEV, *Russian Castings Production* **9** (1975) 365.
18. K. OKABAYSHI, M. KAWAMOTO, A. IKENAGA and M. TSUJIKAWA, *Trans. JFS*, **1** (1982) 37.
19. *Idem.*, *ibid.* **2** (1983) 29.
20. G. F. RUFF and J. F. WALLACE, *AFS Trans.* **85** (1977) 167.
21. J. Y. SU, C. T. CHOW and J. F. WALLACE, *ibid.* **90** (1982) 565.

*Received 3 January  
and accepted 23 August 1989*